



**HAL**  
open science

# The cholesteric defect structure near the smectic A transition

P.E. Cladis, A.E. White, W.F. Brinkman

► **To cite this version:**

P.E. Cladis, A.E. White, W.F. Brinkman. The cholesteric defect structure near the smectic A transition. *Journal de Physique*, 1979, 40 (3), pp.325-335. 10.1051/jphys:01979004003032500 . jpa-00209113

**HAL Id: jpa-00209113**

**<https://hal.science/jpa-00209113>**

Submitted on 4 Feb 2008

**HAL** is a multi-disciplinary open access archive for the deposit and dissemination of scientific research documents, whether they are published or not. The documents may come from teaching and research institutions in France or abroad, or from public or private research centers.

L'archive ouverte pluridisciplinaire **HAL**, est destinée au dépôt et à la diffusion de documents scientifiques de niveau recherche, publiés ou non, émanant des établissements d'enseignement et de recherche français ou étrangers, des laboratoires publics ou privés.

Classification  
*Physics Abstracts*  
 61.30 — 64.70B

## The cholesteric defect structure near the smectic A transition

P. E. Cladis, A. E. White (\*) and W. F. Brinkman

Bell Laboratories, Murray Hill, New Jersey 07974, U.S.A.

(Reçu le 26 juin 1978, révisé le 20 novembre 1978, accepté le 23 novembre 1978)

**Résumé.** — Nous présentons une étude détaillée de la structure des défauts observés près de la transition smectique A — cholestérique dans une géométrie cylindrique. L'orientation des molécules à la surface du capillaire est radiale. On propose que la phase cholestérique apparaisse à partir de la phase smectique A *via* une disinclinaison  $S = + 2$ .

On peut complètement décrire la symétrie d'une phase nématique avec un seul vecteur unitaire,  $\mathbf{n}$ ; par contre, la description de la phase cholestérique nécessite la définition de trois vecteurs mutuellement orthogonaux,  $\mathbf{n}$ ,  $\mathbf{v}$  et  $\mathbf{v} \times \mathbf{n}$ . Bien que le défaut que nous avons observé dans la phase cholestérique à grand pas soit non singulier du point de vue de la configuration de  $\mathbf{n}$ , c'est-à-dire, du point de vue nématique, nous proposons que ce défaut soit singulier dans la phase cholestérique pour laquelle il faut aussi tenir compte des variations de  $\mathbf{v}$  et de  $\mathbf{v} \times \mathbf{n}$ . On présente des arguments d'énergie qui montrent que l'échappement de  $\mathbf{v}$  n'est pas dispersé dans la totalité du volume du cholestérique mais qu'il est concentré dans une région qui est de l'ordre du pas,  $p$ . Ceci nous indique que les défauts d'ordre deux possèdent un cœur, et doivent donc être considérés comme singuliers du point de vue de la phase cholestérique. Cette conclusion est en contradiction avec des arguments topologiques antérieurs appliqués aux cholestériques, qui prédisent qu'un défaut linéaire d'ordre deux doit être non singulier.

**Abstract.** — We study in detail the defect structure observed in a cylindrical geometry near the smectic A-cholesteric transition. The orientation of the molecules at the capillary surface is radial. We propose that the cholesteric phase grows from the smectic A phase *via* a spiralling  $S = + 2$  disclination.

Unlike a nematic which requires only a single unit vector,  $\mathbf{n}$ , to describe completely its symmetry, a cholesteric requires three mutually orthogonal vectors  $\mathbf{n}$ ,  $\mathbf{v}$  and  $\mathbf{v} \times \mathbf{n}$ . We argue that although the defect we have observed is non-singular from the nematic viewpoint, i.e. the configuration of  $\mathbf{n}$  is non-singular, energy considerations imply a core for an  $S = 2$  type line defect for a cholesteric. Specifically, we show that the *escape* of  $\mathbf{v}$  is concentrated in a region of order  $p$ , the pitch, and not dispersed throughout the volume of the material. We interpret this to mean that the  $S = 2$  has a core and therefore must be considered singular from the cholesteric viewpoint. This conclusion disagrees with previous topological arguments which predict for cholesterics that line defects of order two are non-singular.

1. **Introduction.** — Cholesteric liquid crystals are characterized by a twist axis,  $\mathbf{v}$ , perpendicular to the director field,  $\mathbf{n}(\mathbf{r})$ . Ignoring surface contributions, the Frank elastic energy for a cholesteric of volume,  $V$ , is given by [1]

$$F_{el} = \int_V [K_1(\text{div } \mathbf{n})^2 + K_2(\mathbf{n} \cdot \text{curl } \mathbf{n} + q_0)^2 + K_3(\mathbf{n} \times \text{curl } \mathbf{n})^2] dV \quad (1)$$

where  $q_0 = 2\pi/p_0$  is the inverse of the equilibrium

half pitch,  $p_0$ ;  $K_1$ ,  $K_2$  and  $K_3$  are the Frank elastic constants of splay, twist, and bend respectively. In the usual right-handed coordinate system,  $q_0 > 0$  represents a right-handed cholesteric and  $q_0 < 0$  a left handed one. The nematic phase is the special case,  $q_0 = 0$ , so nematics are considered to be cholesterics and there is no known temperature induced nematic-cholesteric transition. This indicates that they are somehow thermodynamically similar despite the different symmetries implied by the two conditions  $q_0 = 0$  and  $q_0 \neq 0$ .

The smectic A phase is characterized by layers.  $\mathbf{n}$ , the same  $\mathbf{n}$  as in eq. (1), defines now the normal to these layers. The layer spacing is of the order of a molecular length  $\sim 25 \text{ \AA}$ . As the temperature decreases in a cholesteric or nematic phase towards a

(\*) Bell Labs. Graduate Research Fellow.  
 Present address : Physics Dept., Harvard University, Cambridge, Massachusetts, U.S.A.

nearly second order nematic/cholesteric-smectic A transition temperature,  $T_{NS}$ ,  $K_2$  and  $K_3$  increase (and are infinite at  $T_{NS}$  should this transition be a continuous one) since twist and bend deformations are excluded by the layered symmetry of the smectic A phase. For a cholesteric, as  $T \rightarrow T_{NS}$ ,  $p_0$  increases. By measuring  $p_0$  as a function of  $(T - T_{NS})$ , one is able to deduce the behaviour of  $K_2$  in the vicinity of  $T_{NS}$  [2]. For a bulk cholesteric, a sufficiently large externally applied magnetic field can successfully compete with the twist free energy to untwist the cholesteric structure [3]. On the other hand, boundary conditions are usually not sufficiently strong except in cases where the sample thickness is less than  $p_0/2$  [4] to untwist the cholesteric but rather result in the introduction of a variety of singular lines.

In this work we study how the cholesteric phase evolves from the well oriented smectic A phase where the layers form concentric cylindrical shells in a capillary so that  $\mathbf{n}$  is initially ( $T \leq T_{NS}$ ) radial and the pitch infinite ( $q_0 = 0$ ). As  $T$  increases, the pitch becomes of the order of the capillary dimension.

As discussed in the next section, we observe a complex sequence of configurations which differ on heating and cooling but which can at least qualitatively be understood in terms of the variation of  $p_0$ ,  $K_3$  and  $K_2$ . One of the more interesting configurations observed appears to have a macroscopic twist in the opposite sense to the cholesteric pitch. We propose that this texture is an  $S = 2$  singular line because such a line has the property of rotating macroscopically in the opposite sense of the local twist. We then propose a texture to describe the escape of the  $S = 2$ . This texture is analytic from the topological point of view of a nematic where only the configuration of  $\mathbf{n}$  is taken into account but singular from the cholesteric viewpoint, where we must also consider two other vectors mutually orthogonal to  $\mathbf{n}$ . We argue that it represents a core (a region where more energy is concentrated) of an  $S = 2$  in a cholesteric which topological considerations [5] indicate should be analytic (the energy is uniformly distributed throughout the material). It is argued here that the topological considerations do not properly take into account the constancy of the pitch in a cholesteric. The importance of an additional constraint due to the constancy of pitch was recognized [6] previously and we apply its ramifications to our case.

Finally we discuss briefly the competing energetics of various configurations near  $T_{NS}$ . We argue that it is the competition between the twist energy and the large value of  $K_3$  that stabilizes the texture containing the  $S = 2$  line. We also discuss the possible role of renormalization of the elastic constants in the presence of bend and twist.

**2. Observations.** — **2.1 SAMPLE PREPARATION.** — Mixtures of CBOOA and CN were prepared in concentrations of 0.1, 0.7 and 1 %. Glass capillaries of

inside diameters ranging from 50 to 400  $\mu$  were filled with these mixtures. The capillaries had been previously treated with the surfactant of Kahn [7] to ensure a homeotropic (i.e. radial) orientation of the director at the inside wall. They were then sandwiched between a glass slide and cover slip and surrounded with microscope immersion oil. The ensemble was placed inside a Mettler oven whose temperature stability is better than 0.02 °C. A varian magnet calibrated by means of an NMR probe was used for the magnetic field experiments. We observed the mixtures using a Leitz ortholux polarizing microscope. The Z axis of the tubes lay always perpendicular to the microscope axis.

**2.2 OBSERVATIONS.** — Only very near the smectic transition temperature did we observe simply two lines in the tube. Generally, we observed at least three and sometimes four lines stretched along the axial direction of the tube. In all cases, at least two of these lines were very sharp dark lines and therefore were presumed singular and identified as either a pair of  $S = +1/2$ 's or  $S = -1/2$ 's. Figure 1 shows the experimental configuration and how it was interpreted (see below).

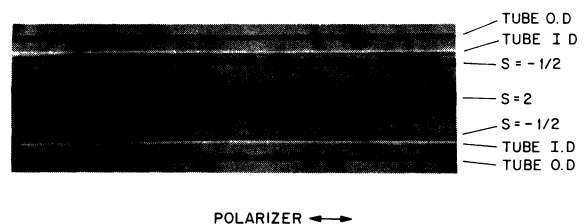


Fig. 1. — The experimental configuration. The axis of the tube is perpendicular to the microscope axis.

We relate here specifically a typical series of observations made on the 0.77 % mixture of CN in CBOOA. Unless otherwise specified, the tube diameter is 133  $\mu$ . The nematic-smectic A transition temperature  $T_{NS}$  was recorded to be 80.8 °C. In general we found that even these small amounts of CN depressed the  $T_{NS}$  of pure CBOOA ( $T_{NS} \sim 83$  °C) by a few degrees but owing to the small quantities of CN involved, we have not attempted to study this quantitatively.

**2.2.1 Heating.** — We first cooled the mixtures into the smectic A phase and observed that the planar  $S = +1$  occurred [8, 9].

Heating very gently (Fig. 2), then, from the smectic A phase where the layers are concentric cylindrical shells [8, 9] ( $S = +1$ ) resulted in the  $S = +1$  splitting into two  $S = 1/2$ 's at 81.0 °C (Fig. 2a).

As the temperature is increased ever so slightly, the two  $S = 1/2$  lines appear to become twisted (Fig. 2b) and at 81.01 °C we observed a new configuration which is shown growing in from the left in figure 2 (b, c and d). This configuration clearly exhibits two singular lines near the wall of the capillary which

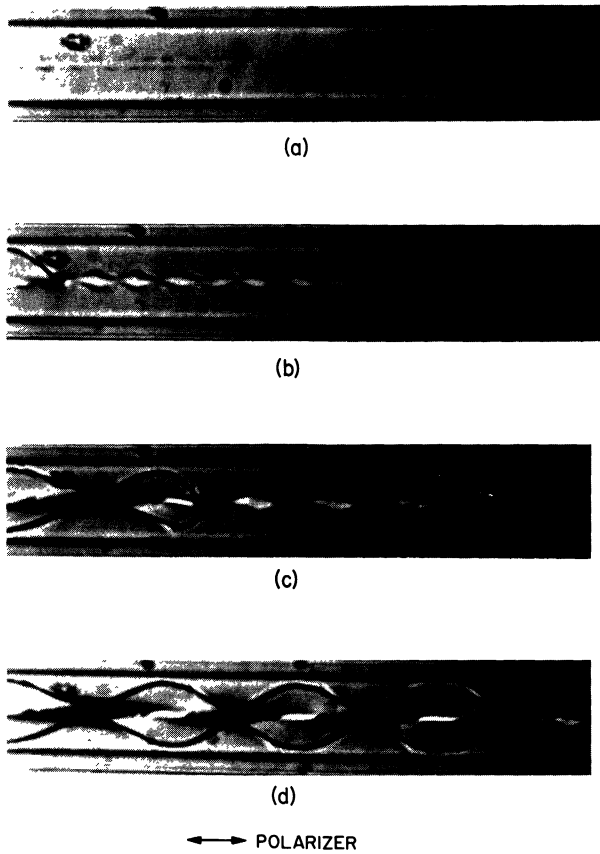


Fig. 2. — Heating very gently from (a) to (d). The  $S = + 1/2$  pair shown in (a) appear as relatively fine lines. When the  $S = 2$  first appears the two  $S = - 1/2$  lines stay close to the centre and appear thickened compared to the  $1/2$  lines in (a). Subsequently (c) and (d) the two  $S = - 1/2$  lines move out toward the walls.

spiral around a bright thick region down the centre. Note that its pitch is considerably different from that of the two  $S = 1/2$ . We propose that this spiraling configuration is a combination of two  $S = - 1/2$  lines near the walls and a non-singular  $S = 2$  line down the centre. On continued heating, the spiral becomes unstable (at 82.5 K) and the result is a proliferation of lines in a very tangled and complex configuration (Fig. 3).

Heating rapidly to 81.01 °C from the smectic phase resulted in the appearance of two  $S = - 1/2$ 's which migrated rapidly to the cylinder walls leaving a thick (non-planar)  $S = + 2$  in the middle of the tube (Fig. 4b). This thick line then proceeded to split into two non-singular  $S = + 1$ 's. Further heating resulted in the  $S = + 1$  pair contorting (Fig. 6 (d-f)) in the middle of the tube but the two  $S = - 1/2$ 's remained perfectly straight. This pattern we have called the *fish scale pattern* (Fig. 4f). The fact that we observed the three line pattern split into the four line pattern is evidence that the non-singular line of the three line pattern is an  $S = + 2$  at least.

We further noted still another configuration on slow heating. This other configuration appears to be related to the spiraling configuration except that the

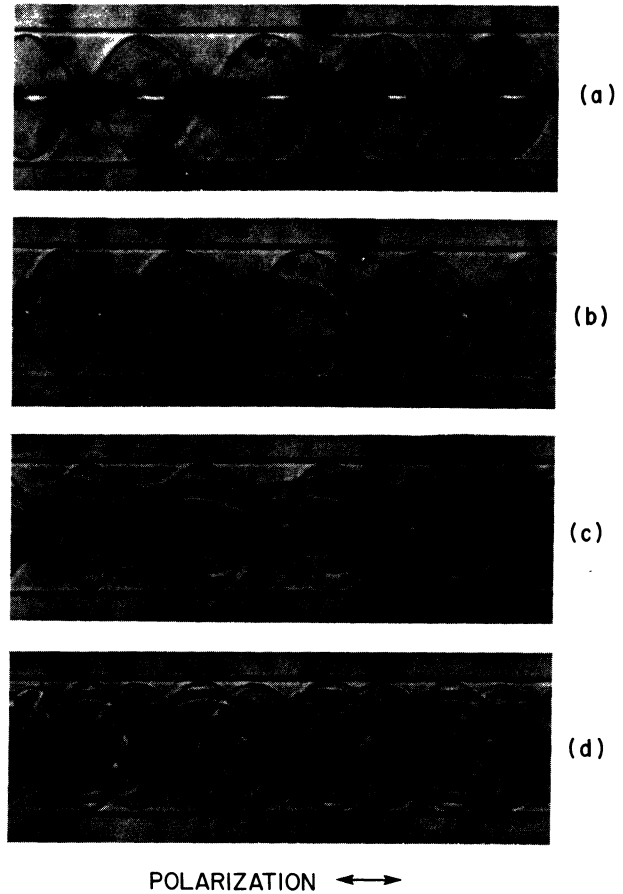


Fig. 3. — Growth of the instability in the spiral pattern as the temperature increases. Note that the spirals first become unstable along the line  $r = 0$ . Temperature increases from a to d.

spiral axis is no longer collinear with the tube axis ( $\hat{z}$  direction) but is tilted with respect to this direction. In figure 5, we show this other pattern growing in from the right with the spirals growing in from the left. When they meet (Fig. 5d), neither configuration gives way indicating that the energies of both configurations are about the same.

In order to understand this spiral texture it is important to note that the sense of the spiral is left-handed. We show this by focussing at various levels in the cylinder (Fig. 6). According to Masubuchi *et al.* [10] CN was found to have *negative twisting power*. They specify that this corresponds to a cholesteric which strongly reflects *left-handed circularly polarized light* or rotates the plane of polarization of transmitted light to the *left* (counterclockwise) *when viewed in the opposite direction to the direction of light propagation*. It thus corresponds to the plane of polarization of the transmitted beam having been turned in a *right-hand sense* by the medium or a right-handed cholesteric [11].

2.2.2 *Cooling.* — If we cool from the very complicated configuration (Fig. 3) we do not recover the spiral. Rather all the cholesteric generated lines are

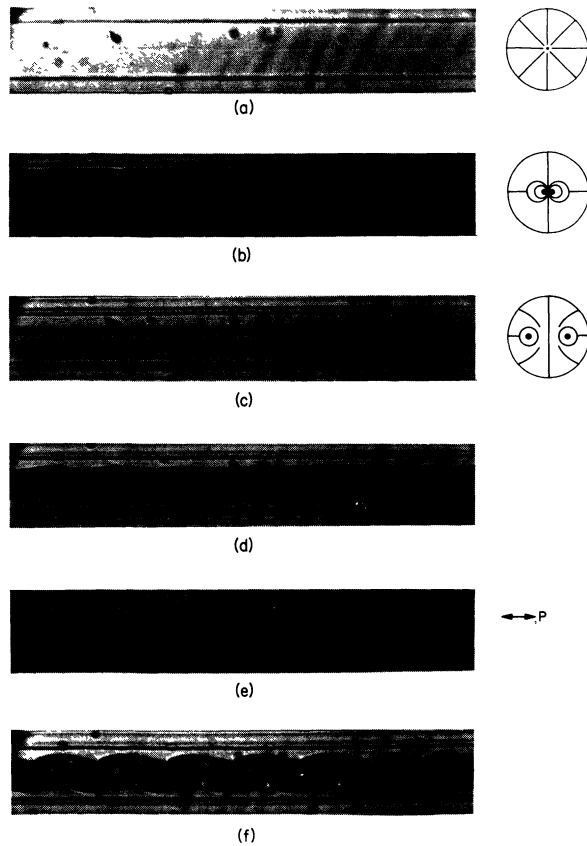


Fig. 4. — Evolution of the fish scale pattern. This pattern was observed on rapid heating from 79 °C (smectic) to 81.1 °C (cholesteric). To the right of the top three photos we show the possible director configuration to account for these lines. Immediately upon becoming cholesteric, two thin lines separate out of the original  $S = + 1$  core and move rapidly toward the walls. The fine  $S = + 1$  core is now replaced by a thick line (b) which we interpret to be an  $S = + 2$  (non-singular). This thick line then proceeds to split into two thick lines (c) which subsequently coil into the fish scale pattern (f). Throughout the two  $S = - 1/2$ 's remain locked on the cylinder surface and do not spiral. P indicates direction of polarizer.

swept in advance of the growing smectic layers and vanish into the core of the smectic  $S = + 1$ .

Cooling the well oriented spirals results in their being compressed without changing their pitch much (Fig. 7).

For the 0.77 % mixture, the spirals were observed to be very stable for  $81\text{ °C} < T < 82.5\text{ °C}$ .

Cooling the fish scale pattern resulted in the straightening of the  $S = + 1$  pair and finally the return of the satellite  $S = - 1/2$ 's to the core of the  $S = + 1$  in the smectic phase (Fig. 8).

2.2.3 Spirals in magnetic field. — a) Perpendicular to tube axis (Fig. 9). — In the geometry, the spirals were observed to behave in a similar fashion to the cooling experiments. The pitch does not change much

Fig. 6. — Monochromatic light. Here we focus successively on the top, middle and bottom of the tube to show that the spirals are both left-handed. ▶

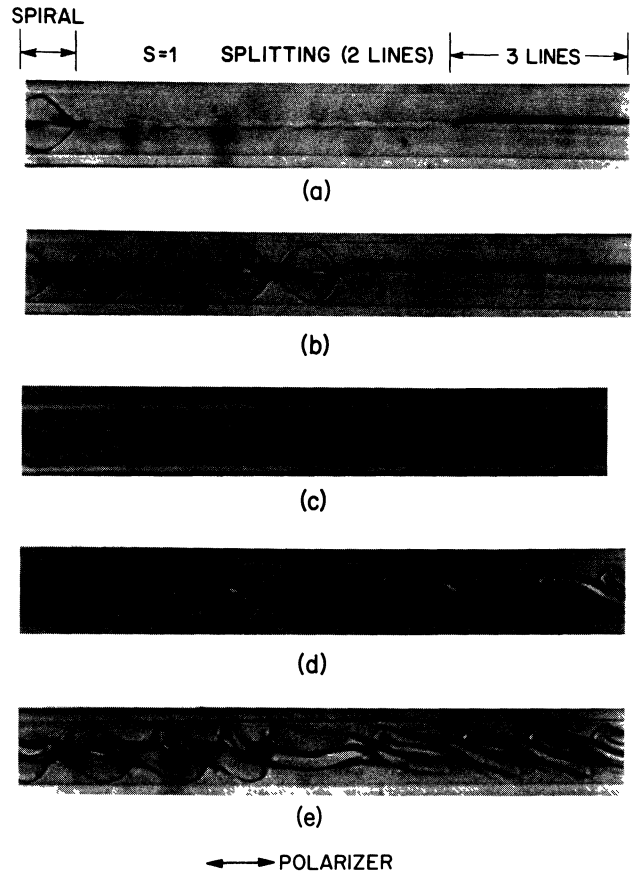
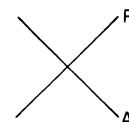
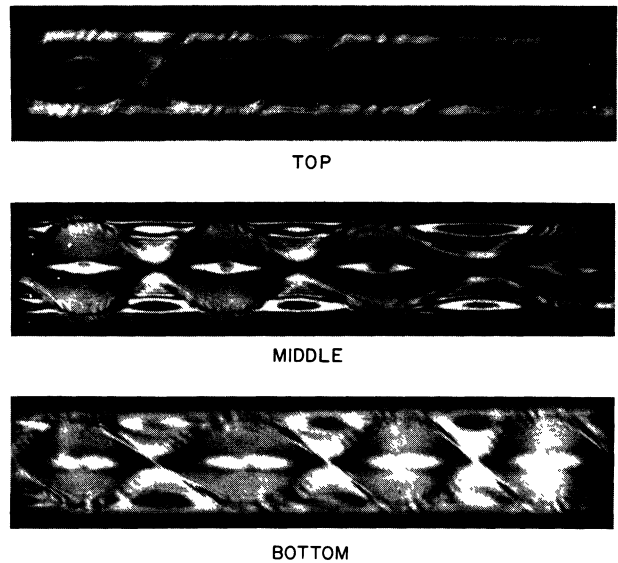


Fig. 5. — The other pattern, which may only be a variation of the spiral pattern, observed on slow heating growing in from the right. When this configuration meets the spiral configuration (b) the point of meeting does not shift indicating that both configurations are of comparable energy. When the spirals become unstable (e) they become indistinguishable from this other configuration.



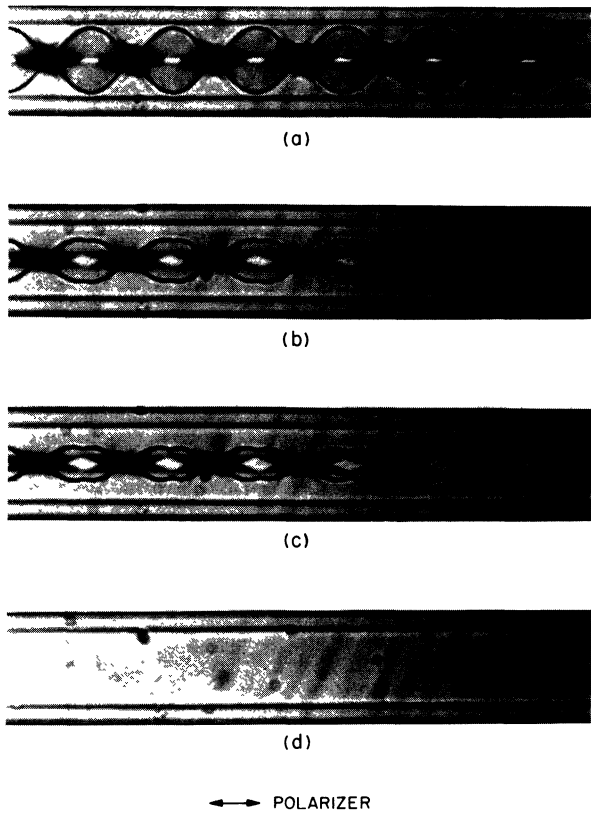


Fig. 7. — Cooling the well oriented spirals back into the smectic A phase. Temperature decreasing from *a* to *d*.

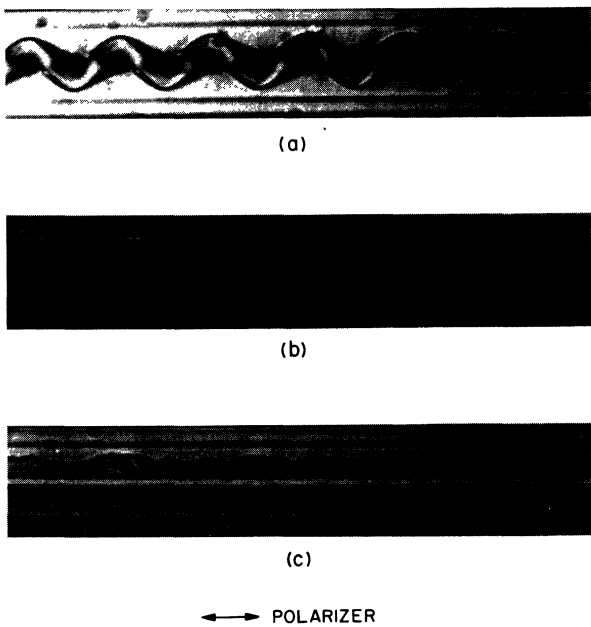


Fig. 8. — Cooling *fish scale* pattern back into the smectic A phase. Temperature decreasing from *a* to *c*. The satellite  $S = -1/2$ 's are difficult to see in this configuration except in (c) where they are seen emerging from the walls and moving toward the centre of the tube. They are slightly blurry here since they move fairly rapidly when they move.

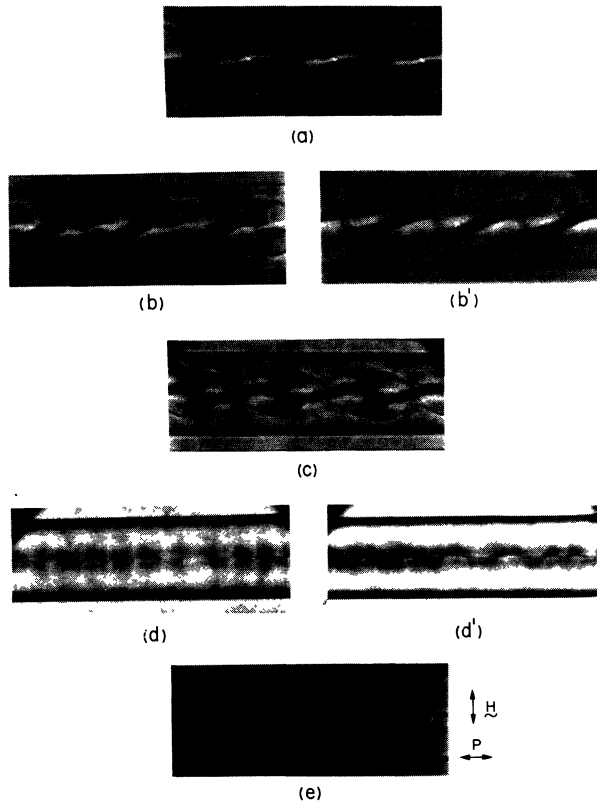


Fig. 9. — Magnetic field applied perpendicular to tube axis *b'* and *d'* are focussed slightly above the plane of *b* and *d*. In *e* the field is about 9 500 G. The magnetic field is increasing from *a* to *e*. For *c*, it is about 7 500 G. Monochromatic light.

(shown figure 9 here to be about  $82 \mu$ ). If anything at about 7 500 G, we observed a slight shrinking of the pitch to about  $75 \mu$  and a sudden straightening of the lines at 9 700 G with the two  $S = 1/2$ 's visible (Fig. 9).

*b) Parallel to tube axis* (Fig. 10). — In this geometry the spiral tilts just before unwinding [4]. Again, the two singular lines are still visible in the centre of the tube. Comparing figure 10c with the *other* configuration of figure 5 shows the similarity between the tilted spirals and the *other* configuration.

*2.2.4 Pitch tube size dependence* (Fig. 11). — There did not appear to be much change in the spiral pitch whenever  $p_0 \gtrsim 2R$  (Fig. 11).

When  $p_0$  was very large compared to the tube diameter we did not observe the close formation of the spirals. Rather, we more generally found three lines stretched out axially. Two of the lines (dark) were quite close to the walls of the cylinder. The middle line was bright. Occasionally we found a region along the tube where the whole configuration twisted just once. The bright middle line suggests again that the  $S = +2$  is of the nonplanar variety ( $n_z \neq 0$ ) and we shall next examine of what sort it might be.

*2.2.5 Contrast of observed micrographs* (Fig. 12). — By analysing the polarization of light emanating from different parts of the pattern, we are able to come to

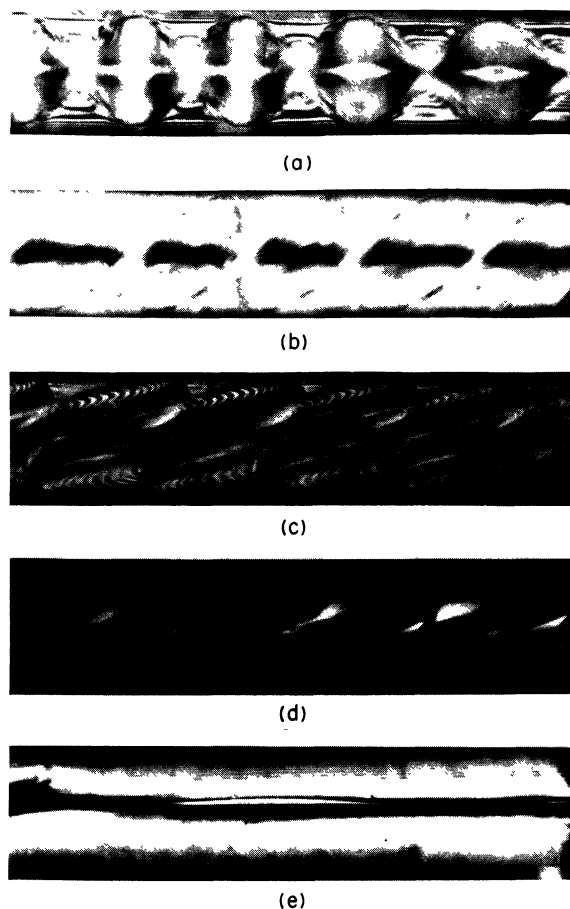
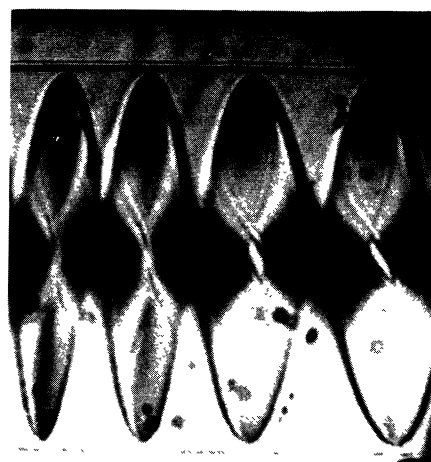


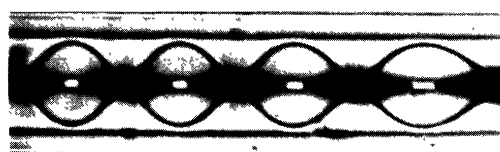
Fig. 10. — Magnetic field applied parallel to the tube axis. The spiral axis tilts just before unwinding. Compare figure 12*b* and *c* with the *other* configuration shown in figures 7*c*-7*e*. The two non-singular lines are difficult to see in 12*e* but are embedded in the black band observed in the middle of the tube. Monochromatic light.

some conclusion concerning the director orientation. To do this, we focus a spot of unpolarized light ( $5 \mu$  diameter) at various levels inside the tube and observe the relative displacement of the « ordinary » or « O » (polarization parallel to the tube axis) to the « extraordinary » or « E » (polarization perpendicular to the tube axis) component of light. This gives an indication of how the director is tilted out of the plane perpendicular to the microscope axis (very roughly) in the plane of focus and below.

In, for example, the scheme of figure 12*a*, we expect the component of the incident beam to be displaced in strictly a radial direction (or not at all). In the other two schemes, it is expected to have an axial component which is different in the two cases. The scheme shown in figure 12*b* predicts a symmetric displacement on diametrically opposite sides of the tube whereas figure 12*c* predicts an asymmetric displacement.



(a)  
TUBE I.D. = 335 microns



(b)  
TUBE I.D. = 85 microns

.77% CN  
←→ POLARIZER

Fig. 11. — Spirals observed in two different tube diameters showing that pitch of spiral is relatively insensitive to the tube diameter.

We have observed the displacement associated with figure 12*c* which leads us to conclude that although the director does *escape*, it does so in a manner which is consistent with a pair of  $\lambda$  like lines rather than by the relatively simple pattern of figure 12*b* which is the Anderson-Toulouse pattern for  $^3\text{HeA}$  [20].

Figure 12*d* shows the director field associated with the helical twisting like pairs in the diametral plane. It is quite regular. We note that when AE is perpendicular to the microscope axis (Fig. 12*d*), four dark extinction lines can be (and are) observed along the direction of the polarizer and analyser crossed at  $45^\circ$  to AE.

Further, the relative displacement of the data is consistent with two right-handed  $\lambda$ 's as we have drawn — additional evidence that the local twist is right-handed everywhere except in the vicinity of the line,  $r = 0$ .

2.2.6 *Summary of observations* (Fig. 13). — Figure 13 summarizes the evolution of the spiral texture.

We mention the *pathological* case we have observed — sometimes the spirals grow independently of each other or they do not grow exactly in phase as we have shown. Eventually, the second spiral catches up without falling out of register with the first spiral. This is a possible growth sequence with this kind of

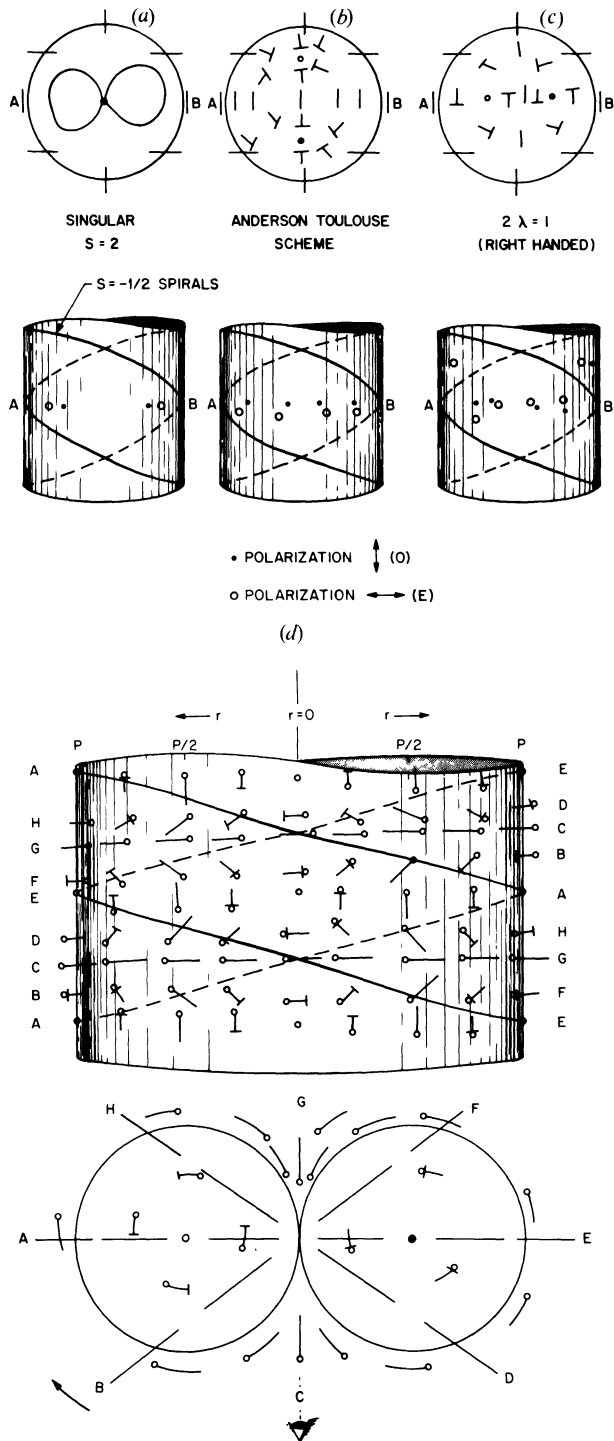


Fig. 12. — a) The singular  $S = 2$  and the expected displacement between the O and E rays. b) Anderson Toulouse scheme [5] for  $^3\text{HeA}$  which is topologically stable and non-singular for three mutually orthogonal vectors. c) A pair of  $\lambda = 1$  for which the relative displacements between the E and O rays are predicted to be opposite to (b). d) The director distribution is shown for (c) both along the  $\hat{z}$  direction and the diametral plane. The lines locate the  $S = -1/2$  pairs which demarcate the lobes of the  $S = 2$ . The scheme on top is what one sees if one is able to focus exactly in the middle of the tube with zero depth of field.

interpretation. Each lobe of the  $S = 2$  need not expand at the same time.

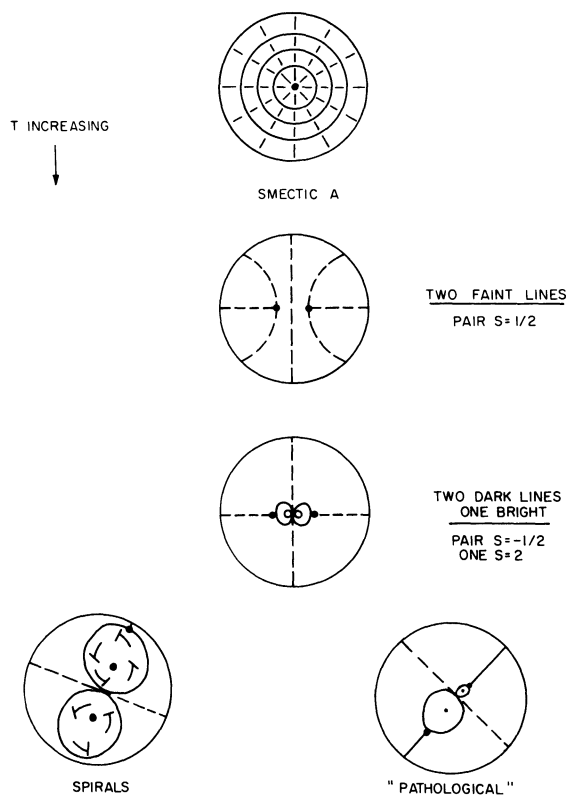


Fig. 13. — Summary of the growth of the spiral texture — also illustrates an observed *pathological* growth.

3. Theoretical considerations and discussion. —

3.1 EQUILIBRIUM PITCH OF MIXTURES. — It is well-known that mixing small amounts of a cholesteric liquid with a pure nematic substance results in a mixture whose twist increases as the concentration of the cholesteric increases. We recall here [4] the simplest way of demonstrating this as a consequence of the equilibrium equations of the Frank free energy.

Let  $q_0$  represent the resulting pitch of the mixture and  $q_c$  the pitch of the pure cholesteric material. The introduction of a small amount of cholesteric into the nematic liquid can be phenomenologically described by a Free Energy

$$F_{el} = K_{2N} q_0^2 V_N + K_{2c} (q_c - q_0)^2 V_c \quad (2)$$

where  $V_N$ ,  $V_c$  and  $K_{2N}$ ,  $K_{2c}$  are the volume and twist elastic constants of the nematic and cholesteric respectively.  $\partial F_{el} / \partial q_0 = 0$  results in

$$q_0 = q_c \cdot \frac{V_c K_{2c}}{K_{2N} V_N + V_c K_{2c}} \quad (3)$$

OR

$$p_0 \cong p_c \cdot \frac{1}{c} \quad (4)$$

where  $c$  is the *weight* concentration of the cholesteric (assuming the densities and elastic constants of the two materials are not very different). This dependence



of the effective pitch of mixtures has been verified in detail by Haas and Adams [12]. From eq. (3) we are able to conclude that the handedness of the twist is expected to be the same as for the pure substance so that a left-handed (dextro rotatory) cholesteric added to a nematic will produce a mixture which is also left-handed.

Since  $p_c$  is usually extremely small,  $\sim 2\,500\text{ \AA}$ – $4\,000\text{ \AA}$ , eq. (3) shows that small amounts of cholesteric added to a pure nematic can result in a cholesteric substance whose pitch  $p_0$  is enormous ( $\sim 50$ – $100\ \mu$ ) and thus more amenable to studies of the defect structure using the simple light microscope. It is these large pitched mixtures which have proven so fruitful in the classification of defects of cholesterics [4]. Here we are also exploiting this feature with the additional property that since  $K_{2N}$  becomes abnormally large near the smectic A transition temperature, the equilibrium pitch of the mixture can become even bigger.

3.2 ENERGETIC CONSIDERATIONS. — 3.2.1 *Renormalization of  $K_{3N}$  and  $K_{2N}$ .* — If the variation of temperature near  $T_{NS}$  only changed the pitch the energetics of the possible configurations might be relatively simple. However, near  $T_{NS}$ , the bend elastic constant  $K_3$  also becomes large so that as the temperature approaches  $T_{NS}$  from above the equilibrium configuration is attempting to eliminate bend and simultaneously increase the pitch. In addition, the onset temperature of the spiral texture is within the region around  $T_{NS}$  in which there are nonlinear corrections to the elastic constants due to the presence of bend and nonequilibrium twist. These corrections act to effectively lower  $T_{NS}$ , and hence,  $K_3$  and  $K_2$  for a given amount of bend or twist. Since the actual values of these elastic constants can be diminished when bend and twist are introduced near  $T_{NS}$ , configurations can occur in this temperature range where bend and twist are not so much minimized as optimized resulting in a total energy (which is the product of the bend elastic constant, say, times some configurational part) is minimum, e.g. the smectic light valve study of Cladis and Torza [13] or the Fredericks transition study of Chu and McMillan [14]. If we assume, the configuration in figure 2d is a non-twisted  $S = 2$ , it is possible to demonstrate that in this case, there is a torque  $\sim K_2^0 \left( \frac{q - q_0}{q} \right)^2$  which twists the  $S = 2$  axially.  $q_0$  is the non-zero equilibrium twist above  $T_{NS}$  and  $K_2^0$  is the bare twist constant.  $q$  is initially ( $T \sim T_{NS}$ ) zero! So, in this range, and in this range only, a not inconsiderable torque is present to wind up an  $S = 2$  axially.

Given the lack of exact solutions to the molecular field equations in this complex geometry we will only make qualitative arguments which allow us to identify the spiral configuration as an  $S = 2$  (or essentially two  $\lambda$  like lines of a cholesteric).

3.2.2 *Configuration energy.* — The first point we discuss here is : why doesn't the simple pair of  $S = 1/2$ 's (Fig. 14) twist (twisting now with the same sense as  $q$ ) helically about  $\hat{z}$ ?

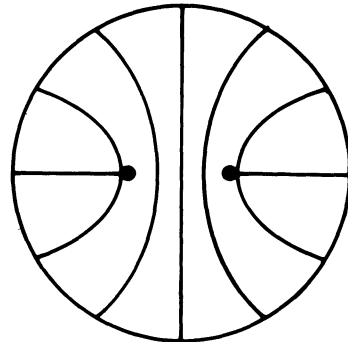


Fig. 14. — View of a pair of  $S = 1/2$ 's. In a cholesteric we can imagine this pair twisting helically in an axial direction. This does not occur near  $T_{NS}$  (see text).

The reason appears to be the following : in order to maximize the gain in twist energy, the  $S = 1/2$  pair must maximize their radial separation,  $R$ . When the  $S = 1/2$  pair is close together, ( $R$  is small), the dominant energy mode is splay. Twisting such a pair will result in a reduction in the twist energy but only in the cylindrical volume around which the lines wrap  $\sim K_2(R/p)^2$ . This increases their length, however, and that contributes an increase in energy

$$\sim \frac{K_1}{2} (R^2/p^2) \ln R/\delta,$$

where  $\delta$  is a core radius  $\sim$  a molecular dimension. The increased length of the lines can overcome the energy gained *via* the twist so that on immediately entering the cholesteric phase the two  $1/2$ 's will not necessarily twist. In addition, the two  $1/2$ 's stay close together to eliminate bend and separating them by a large amount leads to a large addition of bend. Thus what is needed is a texture which puts in the twist but also keeps the amount of bend small.

Transforming to the topologically equivalent  $S = -1/2$  pair and introducing an  $S = 2$  in the small cylinder of radius  $R$ , releases enough bend energy to enable the singular pair to maximize their separation and also to increase their length as they follow the rotation of the  $S = 2$  lobes.

We now consider the configuration energy for the  $S = 2$  as compared to our proposed scheme of a rotating pair of  $\lambda_1$ 's. Clearly, the planar  $S = 2$ , rotating or not, has a singular core from the nematic viewpoint and thus has an energy that is logarithmic in its radius. In contrast, the  $\lambda_1$  pair is not singular even if it is helically twisted in the opposite sense of  $q_0$ .

In cylindrical coordinates,  $(\hat{r}, \hat{\phi}, \hat{z})$  we take for  $\mathbf{n}$  the components,  $n_r = \sin(\varphi + qz)$ ,

$$n_\phi = \cos(\varphi + qz) \cos \theta(r),$$

$n_z = \cos(\varphi + qz) \sin \theta(r)$ . We put  $\theta(r) = qr$  and  $0 \leq \theta \leq \pi$ . This describes our drawing, figure 12d. We get for the total energy per unit length of this line

$$F = \pi[0.27 K_1 + 1.58 K_2 + 1.76 K_3] \quad (5)$$

where  $q = 0.76 q_0$  minimizes the twist free energy. The most significant fact is that the total energy is finite, not sensitive to  $p$  and is reasonably small.

For this configuration, the twist is given by

$$\mathbf{n} \cdot \text{curl } \mathbf{n} = q \cos \theta - \frac{\sin \theta}{r} + \cos^2(\varphi + qz) \times \left[ -q + \frac{\cos \theta \sin \theta}{r} \right]. \quad (6)$$

On the line  $r = 0$  ( $\theta = 0$ ),  $\mathbf{n} \cdot \text{curl } \mathbf{n} = 0$ ! The core of the helical pair of  $\lambda'$ 's is twisted in exactly the opposite sense to the equilibrium pitch but along a radial direction the director twists in the correct sense. *Where they meet, the twists cancel!* For  $\theta = \pi$ , the twist is at least in the correct sense since rotating the  $\lambda$  pair in the opposite sense to  $q$  (i.e. a left-handed sense),  $\mathbf{n}$  twists locally in the proper sense, (i.e. right-handed). This is shown in figure 15.

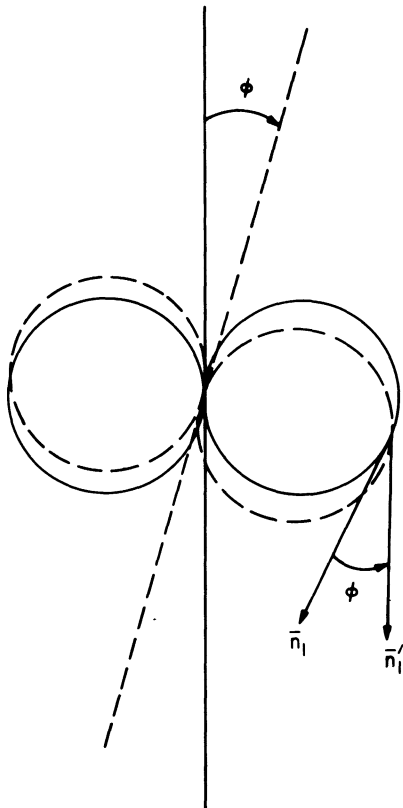


Fig. 15. — Demonstrates that the lobes of a spiralling  $S = 2$  pattern will effectively rotate in a sense contrary to the local twist.

**3.3 HOMOTOPIC GROUP CONSIDERATIONS.** — Recently, Volovik and Mineyev [5] have applied homotopic group theoretical arguments to the case of cho-

lesteric liquid crystals. They concluded that cholesteric liquid crystals belong to the same group as the biaxial nematics of Toulouse [15] and Mermin [16], so that the line singularities are classified by the non-Abelian group which has a unique two dimensional representation the eight element group  $\pm i$  times the Pauli spin matrices. There should thus be five classes of topologically stable line singularities. In contrast, there are no topologically stable point defects. All line defects within the same class can be continuously transformed into each other (i.e. are topologically equivalent). Table I shows their identification of the cholesteric defects along with their class multiplication table.

Table I. — *The class multiplication table and the defect assignments of Volovik and Mineyev [15] for cholesterics.*

$C_0$	$\bar{C}_0$	$C_x$	$C_y$	$C_z$	
$C_0$	$\bar{C}_0$	$C_x$	$C_y$	$C_z$	$C_0$
Class	$C_0$	$C_x$	$C_y$	$C_z$	$\bar{C}_0$
	$C_0 + \bar{C}_0$	$2 C_z$	$2 C_y$	$2 C_x$	$C_x$
	Multiplication		$C_0 + \bar{C}_0$	$2 C_x$	$C_y$
Abelian				$C_0 + \bar{C}_0$	$C_z$
$C_0$	$\bar{C}_0$	$C_x$	$C_y$	$C_z$	
$\chi_0$	$\lambda_1$	$\lambda_{1/2}$	$\tau_{1/2}$	$\chi_{1/2}$	(Or edge or screw dislocations of $p/2$ )
$\lambda_2$	$\tau_1$	$\lambda_{-1/2}$	$\tau_{-1/2}$		
$\tau_2$	$\chi_1$				
$\chi_2$	$S_1$				
(Edge or screw dislocations of $2p$ )	(Edge or screw dislocations of $p$ )				

We remind the reader that  $\lambda_j$  configurations are those where although there is no singularity in the director configuration,  $\mathbf{n}$ , the twist axis  $\mathbf{v}$  which is perpendicular to  $\mathbf{n}$  rotates by  $\pm j 2\pi$  where  $j$  is  $\pm 1/2, \pm 1$ . For a nematic,  $\lambda$  configurations are not line singularities and are topologically similar to the uniform texture. In particular a  $\lambda_1$  configuration in a nematic is an *escaped*  $S = 1$  line [17] and is not singular. On the other hand, for cholesterics  $\lambda'$ 's are distinct from the identity and have a nematic like core on the scale of  $q^{-1}$  because within this distance from the

line  $\mathbf{v}$  is not defined.  $\tau_j$  configurations imply both a singularity in  $\mathbf{n}$  as well as  $\mathbf{v}$ .  $\mathbf{n}$  is parallel to the line singularity in the case of  $\lambda'$ 's and perpendicular to the line in the case of  $\tau'$ 's. In both cases, the twist axis is perpendicular to the line. For  $\chi$  singularities,  $\mathbf{n}$  is perpendicular to the line and is singular whereas the twist axis is parallel to the line and everywhere defined. Volterra type arguments predict that  $\lambda'$ 's and  $\tau'$ 's are necessarily straight line singularities whereas  $\chi'$ 's can adopt any shape [18].  $\lambda'$ 's,  $\tau'$ 's and  $\chi'$ 's are predicted [5] to combine in the manner shown in the class multiplication table (Table I). For example, from the class multiplication table, a member of  $C_x$  ( $\lambda_{1/2}$ , say) added to an element of  $C_y$  ( $\tau_{-1/2}$ , say) can produce either an edge or a screw dislocation or a  $\chi_{1/2}$  (which are members of  $C_z$ ). This, of course, is well-known to be the case for cholesterics and was, in fact, predicted to be so by Frank, Friedel and Kléman [18] before  $\lambda'$ 's,  $\tau'$ 's and  $\chi'$ 's were properly identified. Amusingly, Toulouse has remarked [15] that the classes  $C_x$ ,  $C_y$  and  $C_z$  are the classes of the group for quarks.

As far as we know the class multiplication table of Mineyev and Volovik works for  $\lambda'$ 's,  $\tau'$ 's and  $\chi'$ 's of order 1 or less. We now present arguments that lead us to believe that it *fails* for the combination of two order 1 lines. From the table, two order 1 lines (a pair of  $\lambda'_1$ 's, say) should combine to produce a texture which is topologically equivalent to the identity or uniform texture. Next, we will show that in trying to transform the  $S = 2$  smoothly to a non-singular texture (*making the  $S = 2$  escape*) the escape will be concentrated in a volume on the scale of a pitch (i.e. core) rather than dispersing into the (usually) much larger volume of bulk cholesteric dimensions which is characteristic of non-singular textures.

The essential new results obtained from the topological arguments is that all lines of order one —  $\lambda_1$ ,  $\chi_1$  and  $\tau_1$  are equivalent and that all lines of singularity index greater than one can be mapped back into the lower order lines. In particular, all  $S = 2$  lines are equivalent to the identity so that they must be capable of escape, i.e. their energy must be uniformly spread over the volume of the material and not concentrated in a particular region called the core. These facts are the basis for the discussion by Stein *et al.* [6] of the texture observed in spherulites in terms of the boojum texture proposed for  $^3\text{He}$  [19].

The texture discussed above for our experiments is not legitimately a cholesteric texture in that bend and splay occur on the scale of the pitch so that it becomes difficult to define  $\mathbf{v}$  particularly when  $r \rightarrow 0$ . The present texture is best thought of as an escaped  $S = 2$  in which the escape is occurring in a non-cholesteric core. We could easily generalize it to a legitimate cholesteric texture by recognizing that  $\mathbf{n}(\mathbf{r})$  in figure 12d was constructed by the operations

$$\mathbf{n}(\mathbf{r}, z) = R(\hat{z}, qz) R(\hat{R}(\hat{z}, qz) \hat{r}, \theta(r)) \hat{y} \quad (7)$$

where  $R(\hat{z}, qz)$  is the three dimensional rotation matrix with  $\hat{z}$  the axis of rotation and  $qz$  the rotation angle. In the above calculation we took  $\theta(r) = qr$ . However, note that  $\mathbf{n}(\mathbf{r}, z)$  can also be written as

$$\mathbf{n}(\mathbf{r}, z) = R(\hat{r}, \theta(r)) R(\hat{z}, qz) \hat{y}. \quad (8)$$

Here the final rotation matrix creates the uniform cholesteric while the second describes the deformation of the cholesteric. This way of writing  $\mathbf{n}$  allows an immediate generalization to a legitimate cholesteric texture if we assume that  $\theta(r) = q'r$  and

$$q' \ll q = 2\pi/p_0.$$

The variable  $q' = \pi/R$  where  $R$  is the radius of the core region in which the escape occurs. Normally the energy of such an *escaped* texture would be a constant independent of  $R$  and the escape would spread to fill as large a region as possible. Here, however, the free energy takes the form

$$F = a(qR)^2 + b(qR) + c \quad (9)$$

where  $a$ ,  $b$ , and  $c$  are combinations of elastic constants, and  $a$  is greater than zero. Thus, the minimum energy has  $R \propto q^{-1} = p_0/2\pi$  and the escape is energetically forced into a region the size of the pitch, i.e. a core region (again this statement is made from a cholesteric point of view).

Since this is a variational calculation one might suspect that a better trial function would allow the escape to occur on a more global scale. We do not believe this to be the case at least for the particular type of  $S = 2$  line considered here, that is, a line that at large distance has

$$\mathbf{n}(\mathbf{r}, z) = R(\hat{r}, \pi) R(\hat{z}, qz) \hat{y}. \quad (10)$$

This statement is based on the fact that to avoid the kinds of energies encountered here one must view the cholesteric twist as a set of planes between which  $\mathbf{n}$  rotates by  $2\pi$  and whose separation must be constant or at least  $\propto 1/R$ . This condition makes it impossible for the  $S = 2$  of the type we are discussing to escape. In fact, from the point of view of layers it is not likely that any escaped  $S = 2$  will exist. Until topological arguments which include the nonlocal constraint of constant  $p_0$  are formulated the complete restrictions will not be understood.

The possibility of constraints due to the nonlocal nature of the pitch was recognized by Stein *et al.* [6] but it was not thought to be important for the  $S = 2$  texture and they proposed that the cholesteric texture observed by Robinson *et al.* [21] in spherulites was analytic inside the sphere in a fashion similar to the escaped  $S = 2$  texture proposed by Anderson and Toulouse [20] for the A phase of superfluid  $^3\text{He}$ . Our arguments indicate that there will be a singular line (again from the cholesteric viewpoint) in the bulk of the liquid in a spherulite. This appears to be consistent with the data [21].

**4. Conclusions.** — In conclusion, we have observed a variety of textures in a tube near the smectic A-nematic transition having a complex behaviour for which we mostly do not have explanations. We have proposed a solution (Fig. 12d) for one of the more interesting (and simple) textures that occur which involves a twisted  $S = 2$  line (e.g. Fig. 2d).

In addition, the conclusions of the foregoing arguments may be a valuable clue in helping us to understand why the simple double spiral collapses so dramatically when the temperature increases to a range where the pitch is now much smaller than the radius of the capillary and the sample is entering a state which is unequivocally dominated by cholesteric

symmetries rather than the quasi-nematic state which occurs in the vicinity of the smectic A transition.

We have found that even though this configuration has a finite free energy it is actually a topologically singular configuration for a cholesteric. In fact, from the arguments presented in the preceding section it is all core (!) since the pitch is on the order of the capillary radius. As soon as the pitch becomes much smaller than this dimension, the simple texture (Fig. 2d) becomes unstable (Fig. 3).

Our conclusion that lines of order two necessarily require a core region in a cholesteric contradicts previous topological arguments that order two lines are non-singular.

### References

- [1] FRANK, F. C., *Discuss. Faraday Soc.* **25** (1958) 29.
- [2] See for example VIGMAN, P. B. and FILEV, V. M., *Sov. Phys. JETP* **42** (1976) 747.
- [3] CANO, R., *Bull. Soc. Fr. Miner.* **80** (1967) 333.
- [4] CLADIS, P. E. and KLÉMAN, M., *Mol. Cryst. Liq. Cryst.* **16** (1972) 1.
- [5] VOLOVIK, G. E. and MINEYEV, V. P., *ZhETF* **72** (1977) 2256.
- [6] STEIN, D. L., PISARSKI, R. D. and ANDERSON, P. W., *Phys. Rev. Lett.* **40** (1978) 1269.
- [7] KAHN, F. J., *Appl. Phys. Lett.* **22** (1972) 386.
- [8] CLADIS, P. E., *Philos. Mag.* **29** (1974) 641.
- [9] CLADIS, P. E. and WHITE, A. E., *J. Appl. Phys.* **47** (1977) 1256.
- [10] MASUBUCHI, S., AKAHANE, T., NAKAO, K. and TAKO, T., *Mol. Cryst. Liq. Cryst.* **38** (1977) 265.
- [11] HARTSHORNE, N. H. and STUART, A., *Crystals and the Polarizing Microscope* (Fourth edition), Edward Arnold (Publishers) Ltd. (London) 1970.
- [12] ADAMS, J. E. and HAAS, W., *Cryst. Liq. Cryst.* **15** (1971) 27.
- [13] CLADIS, P. E. and TORZA, S., *J. Appl. Phys.* **46** (1975) 584.
- [14] CHU, K. C. and MCMILLAN, W. L., *Phys. Rev. A* **6** (1972) 936.
- [15] TOULOUSE, G., *J. Physique Lett.* **38** (1977) L-67.
- [16] MERMIN, N. D., *Lecture Notes*, Cornell (1977).
- [17] CLADIS, P. E. and KLÉMAN, M., *J. Physique* **33** (1972) 591.
- [18] FRIEDEL, J. and KLÉMAN, M., in *Fundamental Aspects of Dislocation Theory*; Simmons, J. A., Dewit, R. and Bullough, R., Editors (Nat. Br. Stand. Publication) 1970.
- [19] MERMIN, N. D., in *Quantum Fluids and Solids*, edited by S. B. Trickey, E. Adams and J. Duffy (Plenum, New York) 1977.
- [20] ANDERSON, P. W. and TOULOUSE, G., *Phys. Rev. Lett.* **38** (1977) 508.
- [21] ROBINSON, C., WARD, J. C. and BEEVERS, R. B., *Discuss. Faraday Soc.* **25** (1958) 29; ROBINSON, C., *Trans. Faraday Soc.* **52** (1956) 571.